

# Supporting information for: Synthesis of a Naphthodiazaborinine and Its Verification by Planarization with Atomic Force Microscopy

Zsolt Majzik,<sup>\*,†,¶</sup> Ana B. Cuenca,<sup>‡,¶</sup> Niko Pavliček,<sup>†</sup> Núria Miralles,<sup>‡</sup> Gerhard Meyer,<sup>†</sup> Leo Gross,<sup>†</sup> and Elena Fernández<sup>\*,‡</sup>

<sup>†</sup>*IBM Research - Zurich, 8803 Rüschlikon Switzerland*

<sup>‡</sup>*Department Química Física i Inorgànica, University Rovira i Virgili, 43007 Tarragona Spain*

<sup>¶</sup>*Both authors have equally contributed to this project*

E-mail: maj@zurich.ibm.com; mariaelena.fernandez@urv.cat

## Synthesis

### General information

Solvents and reagents: Solvents and reagents were obtained from commercial suppliers Sigma Aldrich Co. or AllyChem Co., Ltd. and dried by standard procedures, as specified in "*Purification of Laboratory Chemicals*".<sup>S1</sup> All reactions were conducted in oven and flame-dried glassware under an inert atmosphere of argon, using Schlenk-type techniques. Flash chromatography was performed on standard silica gel (Merck Kieselgel 60 F254 400-630 mesh). Thin layer chromatography was performed on Merck Kieselgel 60 F254 which was

developed using standard visualizing agents: UV fluorescence (254 and 366 nm), potassium permanganate/ $\Delta$  or anisaldehyde solution. NMR spectra were recorded at 300 K on a Varian Goku 400 spectrometer.  $^1\text{H}$  NMR and  $^{13}\text{C}$  NMR chemical shifts ( $\delta$ ) are reported in ppm with the solvent (or TMS) resonance as the internal standard ( $\text{CHCl}_3$ : 7.26 ppm ( $^1\text{H}$ )) and ( $\text{CDCl}_3$ ): 77.16 ppm ( $^{13}\text{C}$ ).  $^{11}\text{B}$  NMR chemical shifts ( $\delta$ ) are reported in ppm relative to  $(\text{CH}_3\text{CH}_2)_2\text{O}-\text{BF}_3$ . Data are reported as follows: chemical shift, multiplicity (d = doublet, t = triplet, m = multiplet), coupling constants (Hz) and integration. High resolution mass spectra (HRMS) were recorded on GC-EI-QTOF-MS. A 7890A gas chromatograph coupled with an electronic impact (EI) source to a 7200 quadrupole time-of-flight mass spectrometer (Agilent Technologies, Santa Clara, USA) was used, equipped with a 7693 autosampler module and a J&W Scientific HP-5MS column (30 m x 0.25 mm, 0.25 mm) (Agilent Technologies, Santa Clara, USA). All these measurements were performed at Servei de Recursos Científics i Tècnics (Universitat Rovira i Virgili, Tarragona). GC-MS analyses were performed on a HP6890 gas chromatograph and an Agilent Technologies 5973 Mass selective detector (Waldbronn, Germany) equipped with an achiral capillary column HP-5 (30 m, 0.25 mm i.d., 0.25  $\mu\text{m}$  thickness) using He as the carrier gas. Solvents for chromatography and recrystallization of **1** were GPR grade and were used without further purification.

## Synthesis of (pin)B–B(dan)

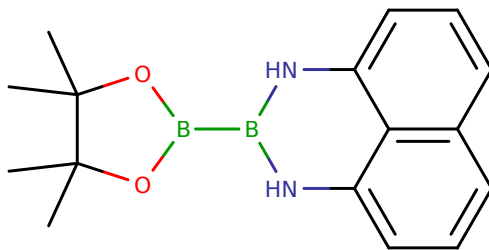


Figure S1: (pin)B–B(dan)

To prepare the mixed diboron reagent (pin)B–B(dan) a slightly modified version of the previously described protocol was used.<sup>S2</sup> Thus Tetrakis(dimethylamino)diboron ( $\text{B}_2(\text{NMe}_2)_4$ )

was synthesized from  $B_2cat_2$  instead of  $BCl_3SMe_2$ . Once prepared the  $B_2(NMe_2)_4$  was sought to react with 1,8-diaminonaphthalene and pinacol in a 1:1:1 ratio in dichloromethane. The slurry was stirred at room temperature for 36 h. After evaporation of volatile materials under vacuum, the solid residue was washed with hot toluene ( $\times 3$ ) to collect washings containing the desired product. After evaporation of toluene from the solution under vacuum, the resultant solid was washed with hexane ( $\times 3$ ). The solid material was dried under vacuum. Following this procedure a global isolated yield of 83 % was attained in a 26.6 mmol scale reaction.

### Synthesis of 9-anthracene naphthodiazaborinine (1)

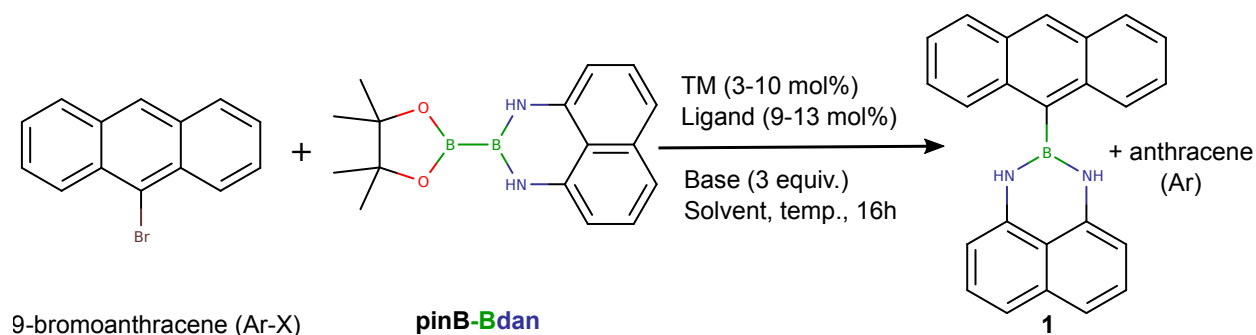


Figure S2

An oven-dried resealable Teflon screw-cap Schlenk reaction tube was evacuated and re-filled with argon; under argon counter flow, (pin)B–B(dan) (1.5 equiv, 0.3 mmol, 88,2 mg), 9-bromoanthracene (1 equiv, 0.2 mmol, 62,2 mg), XPhos (9 mol%, 0.018 mmol, 8.6 mg), KOAc (3 equiv, 0.6 mmol, 58.9 mg), and  $Pd_2(dba)_3$  (3 mol%, 0.006 mmol, 6.25 mg) were added as solids. After evacuation and refill with Argon for three times, dry and degassed 1,4-dioxane (0.86 mL) was added. Then the Schlenk tube was sealed and heated at 100 °C in an oil bath for 16 h. After the reaction was cooled down to room temperature, the obtained mixture was filtered over a Celite<sup>®</sup> small pad and solvent was concentrated on a rotary evaporator. After all the volatiles removed, the crude residue was purified by silica gel flash chromatography to afford **1**.

## NMR

Compound **1**: 2-(anthracen-9-yl)-2,3-dihydro-1H-naphtho[1,8-de][1,3,2]diazaborinine.

Flash column chromatography (standard silica gel), eluent (hexane/EtOAc = 60:1 to 10:1).

Isolated yield **1** (76%). Yellow solid.

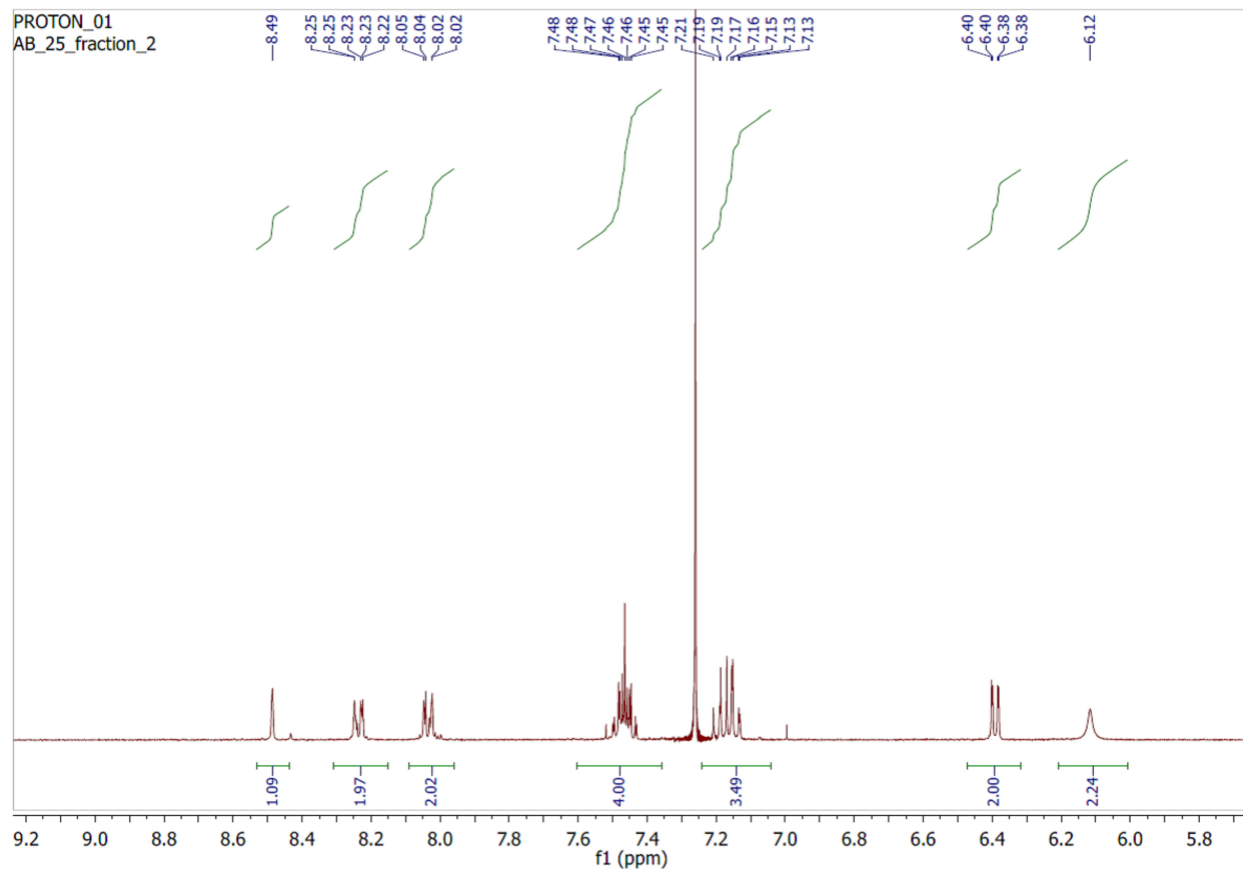


Figure S3:  $^1\text{H}$  NMR of **1** (400 MHz,  $\text{CDCl}_3$ ):  $\delta$  (ppm) 8.49 (s, 1H), 8.24 (m, 2H), 8.03 (dd,  $J = 8.3, 1.5$  Hz, 2H), 7.49–7.43 (m, 4H), 7.21–7.13 (qd,  $J = 8.4, 1.3$  Hz, 4H), 6.39 (dd,  $J = 7.0, 1.3$  Hz, 2H), 6.2 (br, 2H).

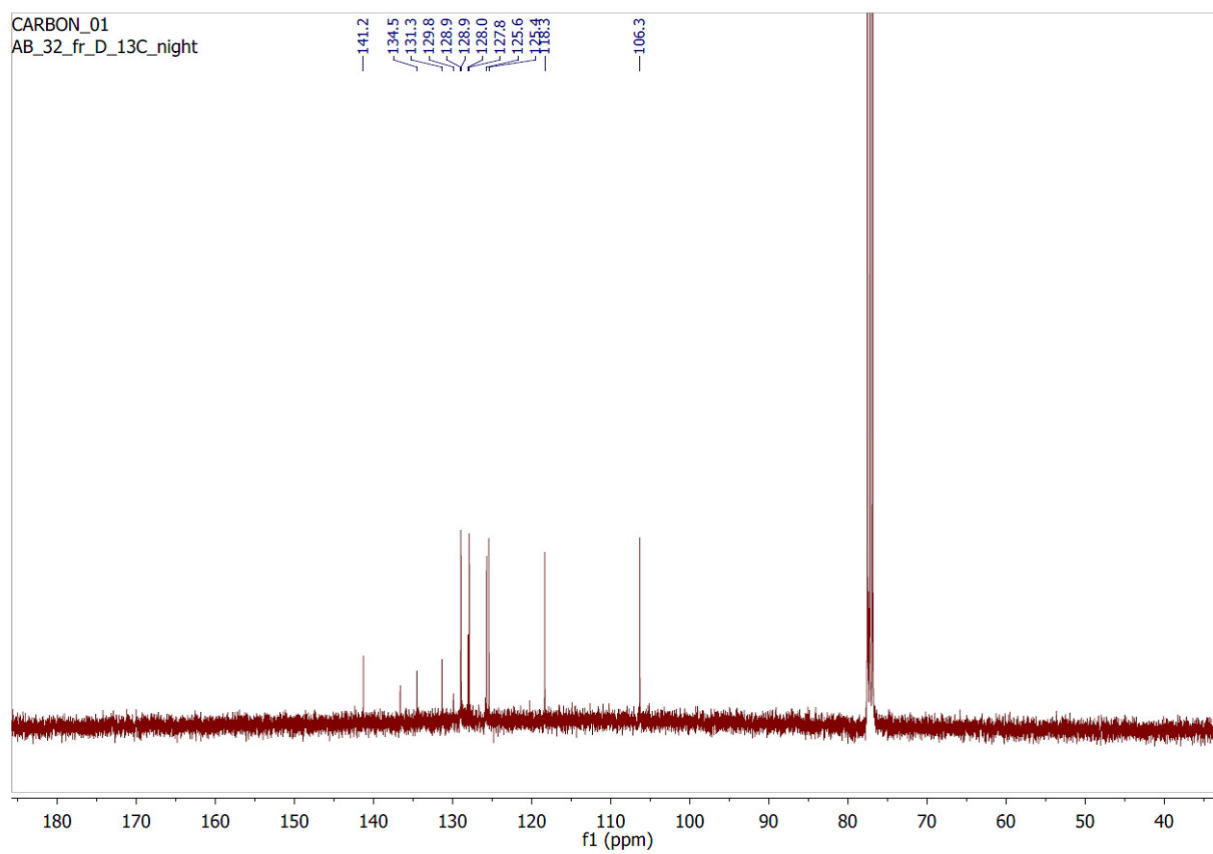


Figure S4:  $^{13}\text{C}$   $\{^1\text{H}\}$  NMR of **1** (125 MHz,  $\text{CDCl}_3$ ):  $\delta$  (ppm) 141.2, 136.6, 134.5, 131.3, 129.8, 128.9, 128.9, 128.0, 127.8, 125.6, 125.4, 118.3, 106.3.

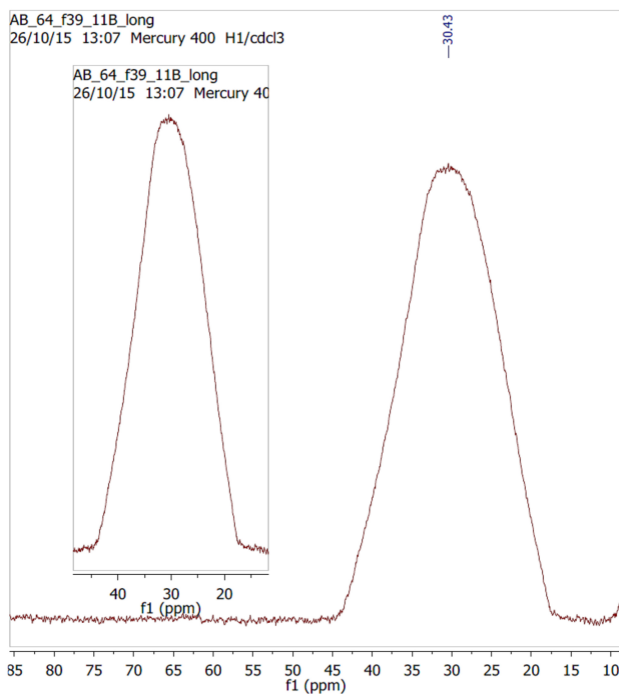


Figure S5:  $^{11}\text{B}$  NMR of **1** (128.3 MHz,  $\text{CDCl}_3$ ):  $\delta$  (ppm) 30.46.

## Cyclic voltammetry (CV)

Cyclic voltammetry experiments of **1** were performed in dry  $\text{CH}_3\text{CN}$  (2 mM),  $[\text{nBu}_4\text{N}][\text{PF}_6]$  (0.1M) as supporting electrolyte (scan rate 100 mV/s) using a Reference 600 Potenciostat – Gamry. A standard three-electrode cell configuration was employed using a glassy carbon working electrode, a platinum-wire counter electrode, and a calomel reference electrode. Formal redox potentials are referenced to SCE.

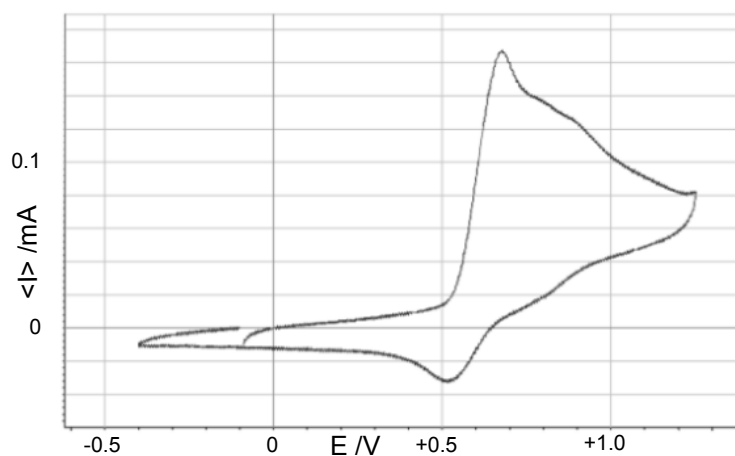


Figure S6: Cyclic voltammetry of **1**. Upon scanning the potential window to below  $-0.5$  V, an essentially irreversible oxidation wave ( $E_{ox} = +0.70$  V (vs. SCE)) is observed.

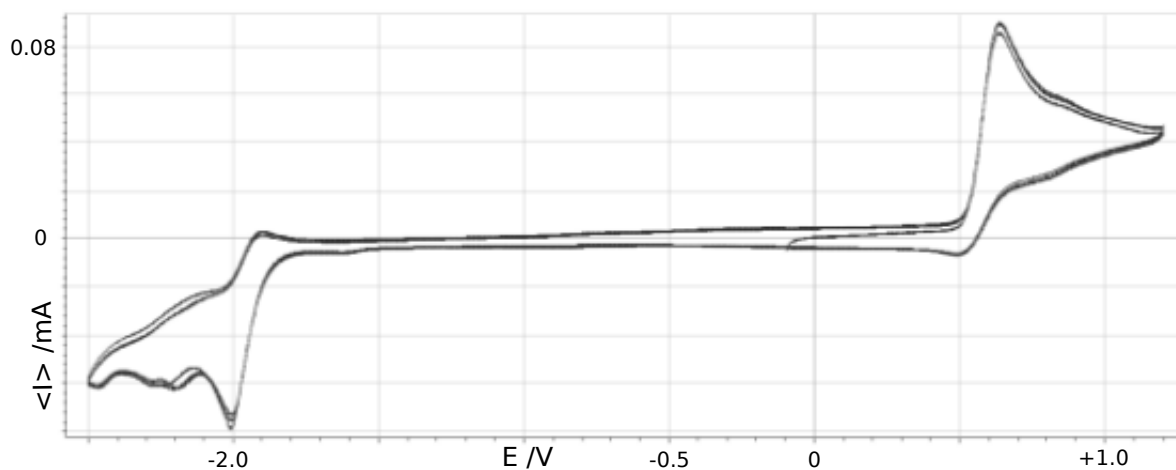


Figure S7: Cyclic voltammetry of **1**. Upon scanning the potential window to below  $-2.5$  V, besides the  $E_{ox} = +0.70$  V oxidation peak, a reduction wave, probably associated to the anthracene fragment of **1**, was observed at  $E_{red} = -2.0$  V. Two consecutive oxidation/reduction potential scans of the event are shown.

# Photophysics

## UV-Vis of compound **1**

UV/vis experiments in solution were performed in quartz square cuvettes of  $10 \times 10 \text{ mm}^2$  (Hellma type 111-QS, suprasil, optical precision). Dry dichloromethane (DCM) was used. Sample concentration:  $10^{-4} \text{ M}$ . Absorption spectra were taken with a UV/vis double-beam spectrometer (VWR UV-6300PC), using the solvent as a reference.

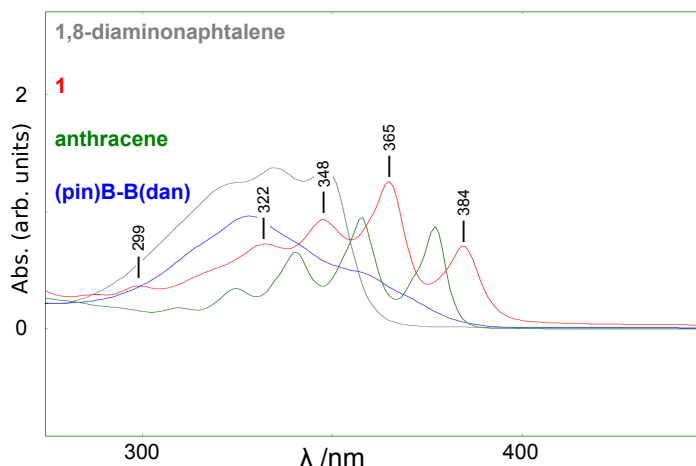


Figure S8: UV/vis of compound **1** (red line), anthracene (green line), (pin)B-B(dan) (blue line) and 1,8-diaminonaphthalene (grey line) measured in DCM.

Significant energy absorptions of compound **1** were observed in the 299 – 384 nm region (see Fig. S8:  $\lambda_{max}$  (Abs.) = 299 (0.3644), 322 (0.7219), 348 (0.9291), 365 (1.2562), 384 (0.7057) nm). Absorption spectra of related anthracene (green line), (pin)B-B(dan) (blue line) and 1,8-diaminonaphthalene (grey line) were also recorded at the same concentration and solvent (dichloromethane, DCM). Based on these comparisons the observed absorption bands are assigned to local  $\pi$  to  $\pi^*$  transitions at the anthracenyl moiety of **1**. All the absorption bands suffer a bathochromic red-shift of about 7 nm if compared to the corresponding anthracene absorptions. This fact might suggest a certain degree of influence of the Bdan unit of **1** upon the  $\pi$  system of the anthracene substituent, including likely higher degree of electronic delocalization.



## Fluorescence emission and excitation spectra of compound **1**:

All fluorescence spectra were obtained on a Fluorolog Horiba Jobin Yvon spectrofluorimeter equipped with photomultiplier detector, double monochromator and Xenon light source. Excitation and emission slits were set at 2 nm for anthracene and 3 nm for the rest of spectra. Emission spectrum of compound **1** was recorded at two different concentrations

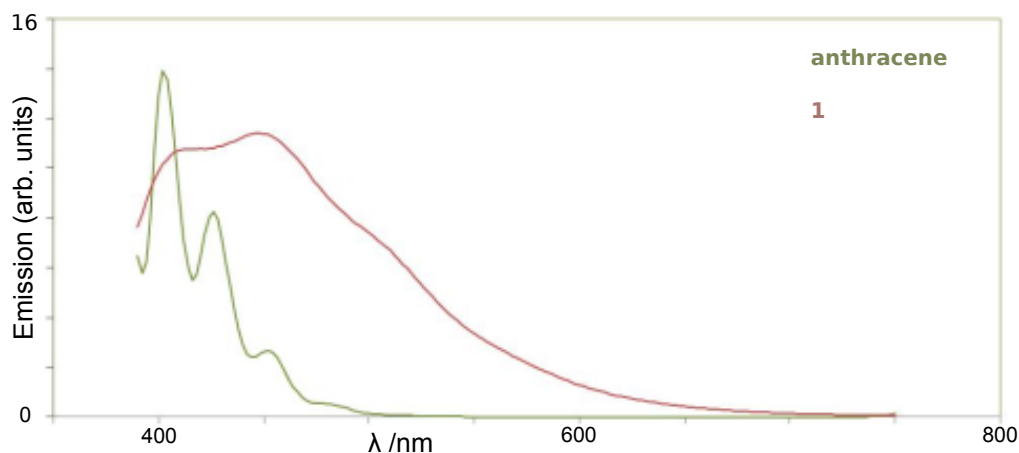


Figure S9: Emission spectra of compound **1** (red line) and anthracene (green line) measured in DCM.

( $10^{-4}$  and  $10^{-5}$  M solution (DCM)). The emission bands, although significantly broadened, show a pattern which is mirror-symmetric with respect to that of the corresponding visible absorption spectrum (see Fig. S9 (red line)). The most intense emission band ( $\lambda_{max} = 427$  nm) arises from a Stokes shift of 62 nm which is larger than the observed value for the parent anthracene (44 nm). To gauge possible contribution of the Bdan fragment to the emission spectra of **1**, we recorded the emission spectrum of the related (pin)B-B(dan). In this case, no significant emission was observed.

Based on the photophysical data presented here it can be concluded that the presence of the Bdan unit effectively modifies the electronic behavior of the anthracene core. The data are as well coherent with the photophysical behavior of other related N-B-N modified aromatic systems investigated for their designed as useful scaffolds for organic thin-film transistor<sup>S3</sup> and dye applications.<sup>S4</sup>

# DFT Calculations

The DFT calculations were performed using the FHI-AIMS code.<sup>S5</sup> The geometry of the isolated molecule was optimized with the tight basis defaults. For structural relaxation the Perdew-Burke-Ernzerhof (PBE) exchange-correlation functional was applied<sup>S6</sup> with vdW correction.<sup>S7</sup> The convergence criteria for the total forces was  $10^{-3}$  eV/Å and for the total energy it was set to  $10^{-5}$  eV.

Within the framework of the Tersoff-Hamann theory, the STM orbital image measured with a metal tip is comparable with the calculated eigenstate densities.<sup>S8,S9</sup> In both reaction paths presented in Fig. 2 two degenerated singly occupied molecular orbitals (SOMO) are formed by dehydrogenation (see Table S1). To take into account the impact of the degeneracy on the observable orbital image, the presented densities in Fig. 4 are the sum of the eigenstate densities of the two SOMO states. The eigenstate density was obtained as the square of the wavefunction, which was calculated by the FHI-AIMS code.

Table S1: Spin up and down occupation and eigenvalues for **2** and **3**.

State	Spin up states		Spin down states	
	Occupation	Eigenvalue [eV]	Occupation	Eigenvalue [eV]
Molecule <b>2</b>				
87	1	-5.95	1	-5.95
88	1	-5.61	1	-4.75
89	1	-5.00	0	-4.43
90	1	-4.79	0	-4.32
91	0	-2.64	0	-2.62
92	0	-1.94	0	-1.68
Molecule <b>3</b>				
87	1	-5.67	1	-5.19
88	1	-5.62	1	-4.37
89	1	-5.28	0	-3.59
90	1	-4.35	0	-3.59
91	0	-3.08	0	-2.99
92	0	-1.79	0	-1.80

## References

- (S1) Perrin, D. D.; Armarego, W. L. F. *Purification of Laboratory Chemicals*, 3rd ed.; Pergamon Press, 1988.
- (S2) Iwadate, N.; Suginome, M. J. *Am. Chem. Soc.* **2010**, *132*, 2548.
- (S3) Lu, Y.; Bolaga, A.; Nishida, J.; Yamashita, Y. Synthesis and Characterization of 1,3,2-Diazaboroine Derivatives for Organic Thin-Film Transistor Applications. *Synthetic Metals*. **2010**, *160*, 1884–1891.
- (S4) Liutao, Y.; Liu, Y.; Zhou, X.; Wu, Y.; Ma, C.; Liu, W. Asymmetric Anthracene-Fused BODIPY Dye with Large Stokes Shift: Synthesis, Photophysical Properties and Bioimaging. *Dyes and Pigments* **2016**, *126*, 232–238.
- (S5) Blum, V.; Gehrke, R.; Hanke, F.; Havu, P.; Havu, V.; Ren, X.; Reuter, K.; Scheffler, M. Ab Initio Molecular Simulations with Numeric Atom-centered Orbitals. *Comput. Phys. Commun.* **2009**, *180*, 2175.
- (S6) Perdew, J. P.; Burke, K.; Ernzerhof, M. Generalized Gradient Approximation Made Simple. *Phys. Rev. Lett.* **1996**, *77*, 3865.
- (S7) Tkatchenko, A.; Scheffler, M. Accurate Molecular Van Der Waals Interactions from Ground-State Electron Density and Free-Atom Reference Data. *Phys. Rev. Lett.* **2009**, *102*, 073005.
- (S8) Tersoff, J.; Hamann, D. R. Theory of the Scanning Tunneling Microscope. *Phys. Rev. B* **1985**, *31*, 805.
- (S9) Repp, J.; Meyer, G.; Stojković, S. M.; Gourdon, A.; Joachim, C. Molecules on Insulating Films: Scanning-Tunneling Microscopy Imaging of Individual Molecular Orbitals. *Phys. Rev. Lett.* **2005**, *94*, 086101.